

Neuronal Excitability

# Astrocyte $\text{Ca}^{2+}$ Influx Negatively Regulates Neuronal Activity

Yao V. Zhang,<sup>1,2</sup> Kiel G. Ormerod,<sup>1,2</sup> and J. Troy Littleton<sup>1,2</sup>DOI:<http://dx.doi.org/10.1523/ENEURO.0340-16.2017>

<sup>1</sup>The Picower Institute for Learning and Memory, Department of Brain and Cognitive Sciences, Massachusetts Institute of Technology, Cambridge, MA 02139, and <sup>2</sup>Department of Biology, Massachusetts Institute of Technology, Cambridge, MA 02139

## Abstract

Maintenance of neural circuit activity requires appropriate regulation of excitatory and inhibitory synaptic transmission. Recently, glia have emerged as key partners in the modulation of neuronal excitability; however, the mechanisms by which glia regulate neuronal signaling are still being elucidated. Here, we describe an analysis of how  $\text{Ca}^{2+}$  signals within *Drosophila* astrocyte-like glia regulate excitability in the nervous system. We find that *Drosophila* astrocytes exhibit robust  $\text{Ca}^{2+}$  oscillatory activity manifested by fast, recurrent microdomain  $\text{Ca}^{2+}$  fluctuations within processes that infiltrate the synaptic neuropil. Unlike the enhanced neuronal activity and behavioral seizures that were previously observed during manipulations that trigger  $\text{Ca}^{2+}$  influx into *Drosophila* cortex glia, we find that acute induction of astrocyte  $\text{Ca}^{2+}$  influx leads to a rapid onset of behavioral paralysis and a suppression of neuronal activity. We observe that  $\text{Ca}^{2+}$  influx triggers rapid endocytosis of the GABA transporter (GAT) from astrocyte plasma membranes, suggesting that increased synaptic GABA levels contribute to the neuronal silencing and paralysis. We identify Rab11 as a novel regulator of GAT trafficking that is required for this form of activity regulation. Suppression of Rab11 function strongly offsets the reduction of neuronal activity caused by acute astrocyte  $\text{Ca}^{2+}$  influx, likely by inhibiting GAT endocytosis. Our data provide new insights into astrocyte  $\text{Ca}^{2+}$  signaling and indicate that distinct glial subtypes in the *Drosophila* brain can mediate opposing effects on neuronal excitability.

**Key words:** astrocyte;  $\text{Ca}^{2+}$ ; *Drosophila*; GABA; GAT; Rab11

## Significance Statement

Complex brain functions require precise control of neuronal activity, which is often disrupted in neurologic disorders such as epilepsy. Here, we show that *Drosophila* astrocytes exhibit endogenous spontaneous  $\text{Ca}^{2+}$  oscillatory activity. Acute elevation of astrocyte  $\text{Ca}^{2+}$  suppresses neuronal activity and causes rapid paralysis. This is accompanied by a rapid reduction in the levels of membrane GABA transporter (GAT), a transporter for the inhibitory neurotransmitter GABA. We identify Rab11 as a novel regulator of GAT trafficking that is required for this form of  $\text{Ca}^{2+}$ -dependent astrocyte regulation of neuronal activity. Our study provides new insight into the acute regulation of neuronal activity by glia.

## Introduction

The regulation of excitatory and inhibitory balance is critically important to neuronal circuit output. Mounting evidence indicates that glial cells are key regulators of

neuronal activity. In particular, astrocytes have been suggested to modulate neuronal output via glia-neuron gap junctions (Nedergaard, 1994; Alvarez-Maubecin et al., 2000) or through the release of gliotransmitters, including

Received November 8, 2016; accepted February 28, 2017; First published March 02, 2017.

The authors declare no competing financial interests.

Author contributions: Y.V.Z., K.G.O., and J.T.L. designed research; Y.V.Z. and K.G.O. performed research; Y.V.Z. and K.G.O. analyzed data; Y.V.Z., K.G.O., and J.T.L. wrote the paper.

glutamate, adenosine/ATP, and D-serine (Papura et al., 1994; Henneberger et al., 2010; Harada et al., 2015; Ma et al., 2016). Despite being nonexcitable cells, astrocytes exhibit robust  $\text{Ca}^{2+}$  dynamics (Volterra et al., 2014; Bazargani and Attwell, 2016; Shigetomi et al., 2016). Early work in the field demonstrated that astrocytes could detect released neurotransmitters and initiate slow somatic  $\text{Ca}^{2+}$  waves secondary to  $\text{Ca}^{2+}$  release from internal stores (Cornell-Bell et al., 1990; Dani et al., 1992). However, a key role of this slower astrocytic  $\text{Ca}^{2+}$  oscillatory activity has fallen out of favor following the finding that animals lacking inositol trisphosphate receptor in astrocytes, which lack this type of glial calcium signaling, have relatively normal brain function (Petravicz et al., 2008; Agulhon et al., 2010). More recently, a form of faster, localized microdomain astrocyte  $\text{Ca}^{2+}$  oscillatory activity was discovered (Shigetomi et al., 2010). Such  $\text{Ca}^{2+}$  fluctuations are mainly contributed through influx of extracellular  $\text{Ca}^{2+}$  (Shigetomi et al., 2012; Rungta et al., 2016) and may represent a more important  $\text{Ca}^{2+}$  signaling pathway for astrocytes to regulate neural activity (Shigetomi et al., 2013).

Astrocytes also control neural activity through their function in neurotransmitter uptake. In the “tripartite synapse” model, astrocyte terminals remove neurotransmitters and terminate their action via neurotransmitter transporters (Eulenburg and Gomez, 2010). Astrocyte uptake of GABA, the primary inhibitory neurotransmitter, via GABA transporters (GATs) is critical for proper regulation of the activity of neuronal circuits (Minelli et al., 1996). In humans, mutations in GAT that disrupt GABA uptake are associated with severe forms of epilepsy (Carvill et al., 2015). GAT has been shown to exhibit a very high turnover rate, with a third of the protein residing in a recycling pool (Wang and Quick, 2005), implying that regulation of GAT plasma membrane expression may serve as an acute mechanism to modulate neuronal activity via changes in the rate of GABA uptake. Several factors involved in GAT trafficking have been identified (Scimemi, 2014), but the mechanisms regulating fast turnover of GAT remain elusive.

*Drosophila* has several classes of glial cells (Freeman, 2015). Astrocyte-like glia (hereafter referred to as astrocytes) and cortex glia are the two main subtypes found intimately associated with neurons in the CNS (Kremer et al., 2017). It has recently been shown that *Drosophila* cortex glia exhibit near-membrane microdomain  $\text{Ca}^{2+}$  os-

illatory activity (Melom and Littleton, 2013). Mutations in Zydeco, a glial-specific  $\text{K}^+$ -dependent  $\text{Na}^+/\text{Ca}^{2+}$  exchanger (NCKX), eliminate microdomain  $\text{Ca}^{2+}$  oscillations in cortex glia and lead to higher intracellular  $\text{Ca}^{2+}$  levels. This increase in cortex glial  $\text{Ca}^{2+}$  leads to enhanced seizure susceptibility, as does acute induction of  $\text{Ca}^{2+}$  influx through ectopic expression of TRP channels in cortex glia (Melom and Littleton, 2013). These observations have led to a model whereby increased  $\text{Ca}^{2+}$  influx into cortex glia leads to neuronal hyperexcitability. However, it is unknown whether *Drosophila* astrocytes also exhibit  $\text{Ca}^{2+}$  activity and whether astrocyte  $\text{Ca}^{2+}$  signals have a similar role in exciting neighboring neurons. In the present study, we report that *Drosophila* astrocytes exhibit spontaneous, microdomain  $\text{Ca}^{2+}$  transients, resembling those observed in their mammalian counterparts. Surprisingly, unlike cortex glia, acute  $\text{Ca}^{2+}$  influx in astrocytes causes behavioral paralysis and a rapid loss of neuronal activity. We find this suppression of neuronal activity is due in part to rapid GAT endocytosis from astrocyte membranes, leading to enhanced GABA levels in the synaptic cleft. We identify Rab11 as a key regulator of GAT trafficking downstream of astrocyte  $\text{Ca}^{2+}$  influx and find that reduction in GAT turnover via suppression of Rab11 function ameliorates the induced suppression of neuronal activity.

## Materials and Methods

### *Drosophila* stocks

All *Drosophila* stocks were maintained on standard media at room temperature (22°C). The following stocks were used: UAS-TrpA1 (BDSC 26263), Alrm-Gal4 (Doherty et al., 2009), UAS-Rab11-GFP (BDSC 8506), GAD1-Gal4 (Ng et al., 2002), UAS-Rab11-RNAi [#I, VDRC 22189 (Dietzl et al., 2007); #II, BDSC 27730 (Perkins et al., 2015)], UAS-Rab11<sup>N124I</sup> (Satoh et al., 2005), repo-Gal80 (Awasaki et al., 2008), and elav-Gal80 (Yang et al., 2009). To create a stable UAS-TrpA1-myc line, UAS > stop > TrpA1-myc flies (von Philipsborn et al., 2011) were crossed with  $\beta\text{Tub85D-FLP}$  (BDSC 7196) to excise the transcriptional stop codon. For all experiments, flies of either sex were assayed.

### Generation of transgenic flies

To construct the plasmid pBID-UASc-myrGCaMP6s, GCaMP6s cDNA (Addgene #40753) was PCR amplified by designing primers with restriction enzyme cutting sites added on each end. Plasmid pBID-UASc-myrGCaMP5G (Melom and Littleton, 2013) was digested with NotI and XbaI and ligated with GCaMP6s using standard procedure. Cloning was verified by sequence analysis (Genewiz). To generate transgenic *Drosophila*, plasmids were injected into embryos of a strain with a third chromosome attP docking site (BDSC 8622) by Bestgene.

### Behavioral assays

For testing the temperature sensitive behavioral phenotype of adult flies, 2-d-old flies were used. A total of 10–12 flies were transferred to each vial and placed in a water bath held at the indicated temperature. The number of flies with motor impairment was observed and manually

This work was supported by the HHS/NIH Grant NS40296.

Acknowledgements: We thank Marc Freeman, Tzumin Lee, Yuh Nung Jan, Akiko Satoh, the Developmental Studies Hybridoma Bank at the university of Iowa, the Bloomington *Drosophila* Stock Center at Indiana University, the Vienne *Drosophila* Resource Center, and the *Drosophila* stock center at National Institute of Genetics of Japan for providing reagents and flies strains.

Correspondence should be addressed to Yao V. Zhang at 43 Vassar St, 46-3251, Cambridge, MA 02139. E-mail: yaov@mit.edu.

DOI: <http://dx.doi.org/10.1523/ENEURO.0340-16.2017>

Copyright © 2017 Zhang et al.

This is an open-access article distributed under the terms of the Creative Commons Attribution 4.0 International license, which permits unrestricted use, distribution and reproduction in any medium provided that the original work is properly attributed.

**Table 1: Statistical table**

	Data structure	Type of test	Observed power ( $\alpha = 0.05$ )
a (Fig. 2A)	Non-normal distribution	Mann-Whitney test	1
b (Fig. 3A)	Normal distribution	Student's <i>t</i> test	1
c (Fig. 3B)	Non-normal distribution	Mann-Whitney test	1
d (Fig. 3D)	Normal distribution	Student's <i>t</i> test	0.0838271
e (Fig. 3G)	Non-normal distribution	Wilcoxon signed-rank test	0.2684
f (Fig. 4B)	Normal distribution	Student's <i>t</i> test	0.0975257
g (Fig. 4B)	Normal distribution	Student's <i>t</i> test	0.999942

recorded for up to 5 min, with an interval of 15 s in the first minute and 30 s in the following 4 min. Paralysis of adult flies was defined by complete loss of movement. For RNAi screening conducted at 30°C, *Alrm > TrpA1* flies do not show 100% penetration of the paralysis phenotype. In this case, the number of flies that showed severe motor impairment and were unable to climb up the vial wall were recorded at each time point. For testing the behavior of headless flies, heads of adult flies were severed by fine scissors under CO<sub>2</sub> anesthetization. These flies were then allowed to recover at room temperature in a closed Petri dish for 1 h before being transferred to Petri dishes preheated to the indicated temperature.

#### Immunofluorescence

For immunofluorescence, 3rd instar stage larvae were dissected in HL3.1 (70 mM NaCl, 5 mM KCl, 10 mM NaHCO<sub>3</sub>, 4 mM MgCl<sub>2</sub>, 5 mM trehalose, 115 mM sucrose, and 5 mM HEPES; pH 7.2; [Feng et al., 2004](#)) and fixed for 10 min either in Bouin's fixative or 4% paraformaldehyde. Following washes with PBST (PBS containing 0.1% Triton X-100), larval fillets were blocked for 30 min with 5% normal goat serum in PBST, then incubated with primary antibody overnight at 4°C. Fixed larvae were then washed with PBST. Secondary antibody incubation was performed at room temperature for 2 h. Samples were washed and mounted in vectashield (Vector Laboratories). Antibodies for immunostaining and their dilution were as follows: rabbit anti-GAT, 1:2000 ([Stork et al., 2014](#)); mouse anti-Repo, 1:100, (DSHB 8D12); mouse anti-Brp, 1:100 (DSHB NC82); mouse anti-GFP, 1:500 (Thermo Fisher Scientific 33-2600); DyLight 649-conjugated anti-horseradish peroxidase, 1:500 (Jackson ImmunoResearch); Alexa Fluor 488-conjugated goat anti-mouse, fluorescein isothiocyanate-conjugated goat anti-rabbit; and Alexa Fluor 546-conjugated goat anti-mouse, 1:500 (Thermo Fisher Scientific). Images were acquired on a Zeiss LSM700 Laser Scanning confocal microscope with a 40× 1.3 NA, or a 100× 1.3 NA oil-immersion objective (CarlZeiss).

#### Western blot analysis

Adult flies were snap frozen in liquid nitrogen and five heads per sample were collected and homogenized in 50  $\mu$ l of 1× Laemmli loading buffer (60 mM Tris, pH 6.8; 10% glycerol; 2% SDS; 1%  $\beta$ -mercaptoethanol; and 0.01% bromophenol blue), followed by centrifugation at 16,000  $\times$  *g* for 10 min to clear the homogenate. Supernatant was analyzed by SDS-PAGE (Bio-Rad 456-1086) and transferred to nitrocellulose membrane. Membranes were blocked with blocking buffer (2% bovine serum albumin,

2% nonfat dry milk, 0.02% Tween 20 in TBS) and then incubated with appropriate antibodies for immunoblotting. Primary antibody incubation were performed with gentle shaking at 4°C overnight followed by four 5-min washes using TBS containing 0.01% Tween 20, secondary antibody incubation for 1 h at room temperature, and four more 5-min washes using TBS containing 0.01% Tween 20. Then the membrane was briefly rinsed with TBS, and the blot was visualized using an Odyssey infra-red scanner (Li-Cor). Antibodies for Western blotting: rabbit anti-GAT, 1:5000 (gift from Marc Freeman; [Stork et al., 2014](#)); mouse anti-Tubulin, 1:60,000 (Sigma-Aldrich, clone B<sub>5</sub>-1-2). Alexa Fluor 680-conjugated anti-rabbit and Alexa Fluor 800-conjugated anti-mouse, 1:10,000 (Invitrogen). All antibodies were diluted using blocking buffer.

#### Electrophysiology

Extracellular recordings were obtained from dissected 3rd instar larvae using a fire-polished patch electrode. To record central pattern generator (CPG) activity, the larval brain was left intact and care was taken during dissection to avoid damaging segmental nerves. Recordings were amplified using an AxoClamp 2B amplifier and digitized via an Molecular Devices Digidata 1550 (Molecular Devices). Clampfit 6.1 software was used to record and process electrophysiological data. Larvae were constantly perfused via a gravity system with HL3.1 solution containing 1.5 mM Ca<sup>2+</sup>. Saline was heated using an in-line solution heater (Harvard Apparatus), controlled by a Dual Channel Bipolar Temperature Controller (CL-200A). Additionally, the recording dish was temperature controlled using a Peltier device regulated by a fan-based heat sink and a Dual Channel Temperature Controller (Koolance, Warner Instruments).

#### Live imaging of astrocyte Ca<sup>2+</sup> transients

UAS-*myrGCaMP6s* was expressed in astrocytes using the *Alrm-Gal4* driver. L2 stage larvae were mounted on their ventral side in a small drop of water on a 25  $\times$  60 mm coverslip. A single layer of scotch tape was applied on each side of the larva as a spacer to avoid damaging the animal when an 18  $\times$  18 mm coverslip was placed on top. An upright PerkinElmer Ultraview Vox spinning disk confocal microscope equipped with a high-speed EM CCD camera, and a 43× 1.3 NA oil objective was used for image acquisition. Velocity software was used for data analysis. When imaging, the assembly was flipped so that the ventral side of the larvae faced the objective. Time series were acquired at a speed of ~9 Hz using a single optical plane in the neuropil layer of the larval ventral nerve cord (VNC).

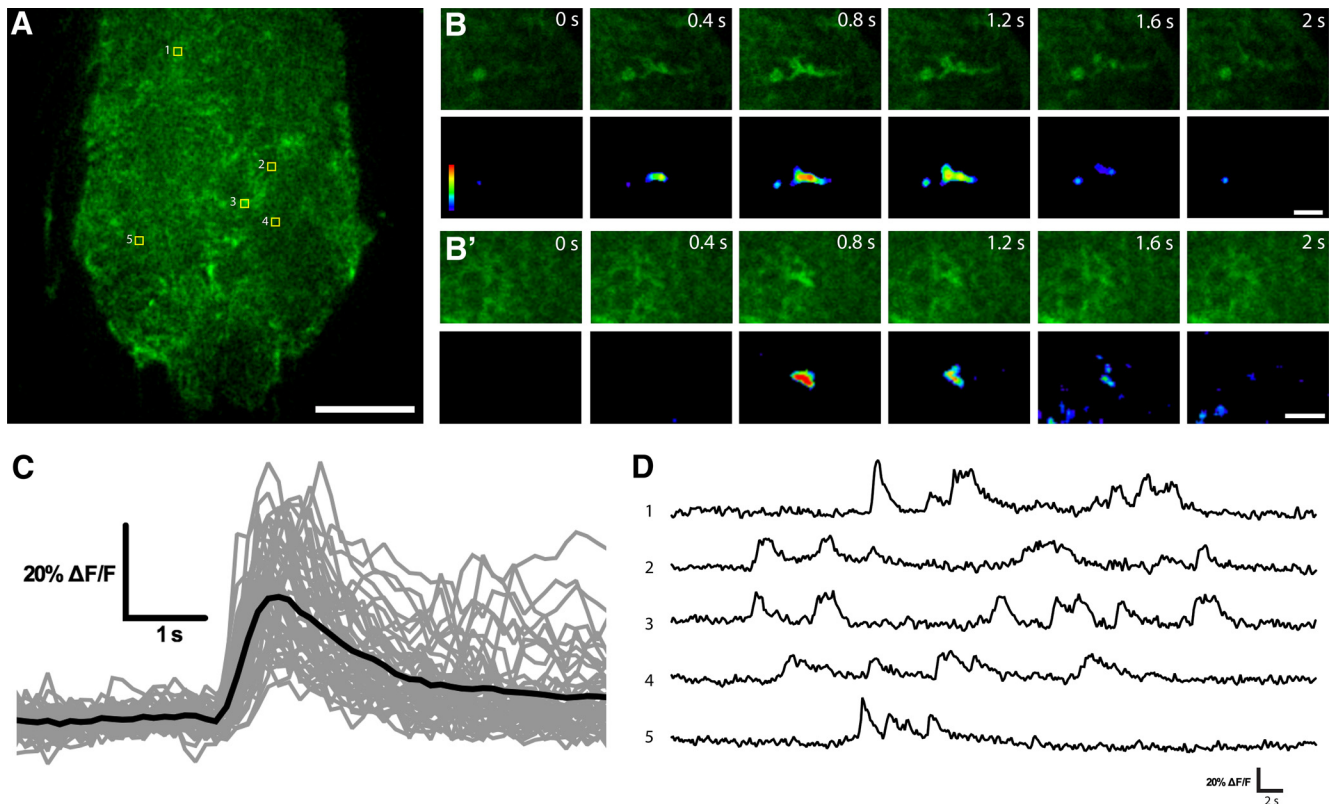


**Figure 1.** Near-membrane  $\text{Ca}^{2+}$  activity in *Drosophila* astrocytes. **A**, Single confocal plane of larvae VNC showing the astrocyte-specific expression of myrGCaMP6s under the control of Alrm-Gal4. **B**, **B'**, Time-lapse image series of two microdomain astrocyte  $\text{Ca}^{2+}$  transients. **C**, Superimposition of astrocyte  $\text{Ca}^{2+}$  traces (in gray) and their average (black line;  $n = 46$  individual traces). **D**, Sample traces of recurring  $\text{Ca}^{2+}$  transients in five different areas indicated in **A**. Scale bars  $20\ \mu\text{m}$  (**A**) and  $5\ \mu\text{m}$  (**B** and **B'**).

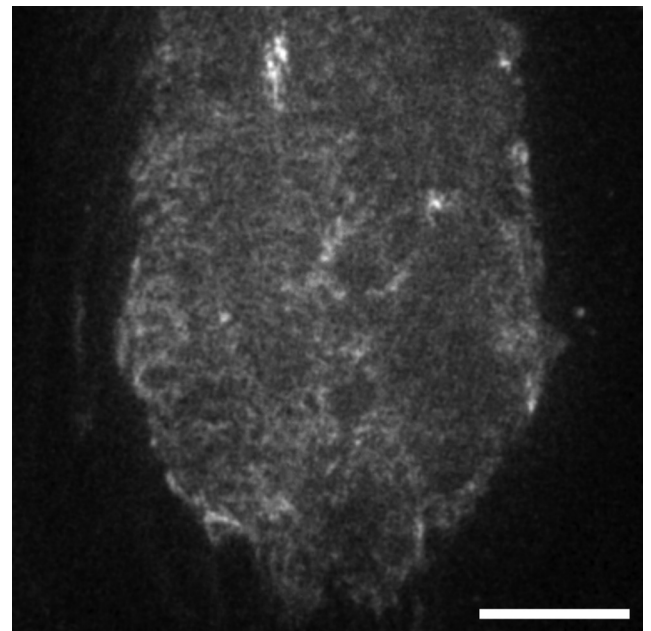
#### Statistical analysis

Statistical analysis was performed using GraphPad Prism 6. Data are presented as mean  $\pm$  SEM in all figures. Statistical analysis is summarized in Table 1. Superscript letters following  $p$  values are used to refer to the corresponding comparisons described in the table.

## Results

### *Drosophila* astrocytes show microdomain $\text{Ca}^{2+}$ transients

Expression of a genetically encoded membrane targeted myristoylated  $\text{Ca}^{2+}$  indicator (GECI) in cortex glia, a type of glia that associate with neuronal cell bodies in the *Drosophila* CNS, has revealed that these cells display robust near-membrane microdomain oscillatory activities (Melom and Littleton, 2013). To determine whether astrocytes, the other major glial cell type closely associated with neurons in the *Drosophila* CNS, show similar  $\text{Ca}^{2+}$  activity, we generated transgenic lines expressing a myristoylated form of GECI, myrGCaMP6s, under the control of an astrocyte-specific promoter, Alrm-Gal4 (Fig. 1A; Doherty et al., 2009). We found that astrocytes display robust spontaneous  $\text{Ca}^{2+}$  oscillatory activity in membrane microdomains of processes that invaded the synaptic neuropil, largely resembling the  $\text{Ca}^{2+}$  transients observed in cortex glia (Fig. 1B; Movie 1). We also monitored astrocyte  $\text{Ca}^{2+}$  activity using standard dissected preparations bathed in HL3.1 saline with up to  $4\ \text{mM}\ \text{Ca}^{2+}$ . Even



**Movie 1.** *Drosophila* astrocyte near-membrane  $\text{Ca}^{2+}$  activity detected with myrGCaMP6s.  $\text{Ca}^{2+}$  transients were recorded from the VNC of undissected 2nd instar larvae. Video speed,  $2\times$  real time. Scale bar,  $20\ \mu\text{m}$ .



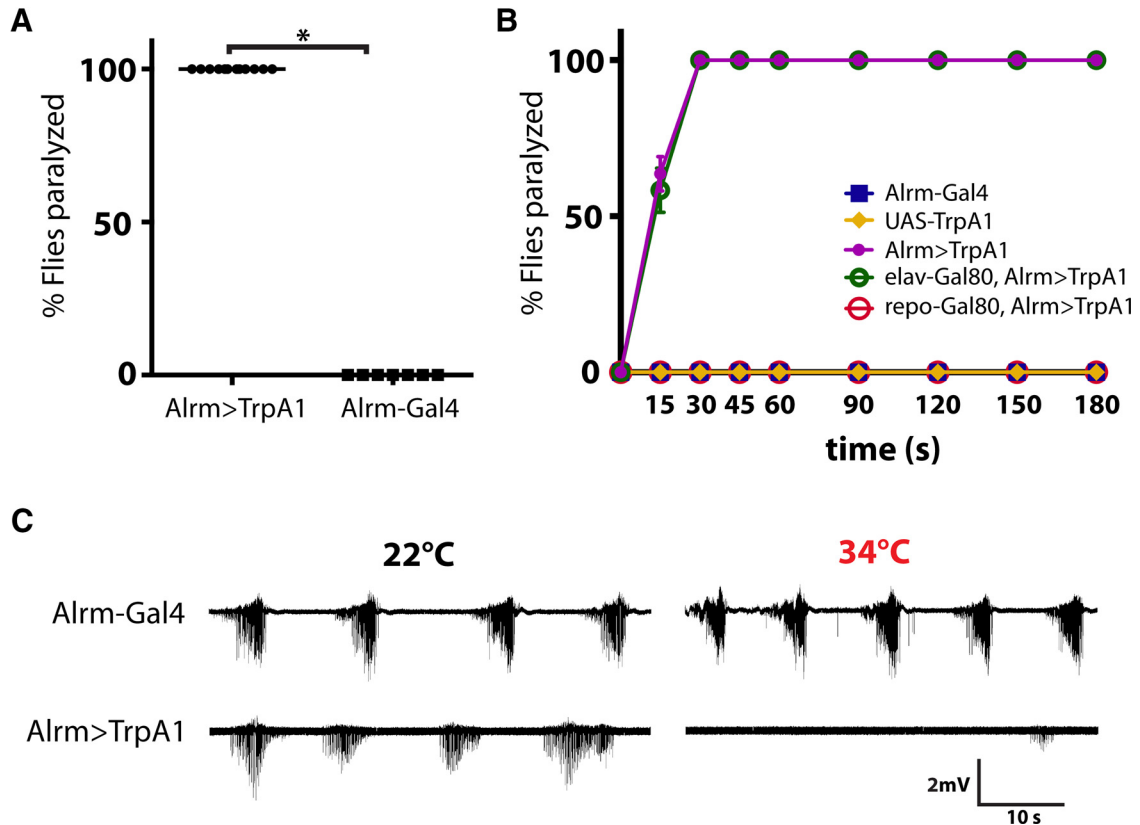


**Figure 2.** Acute astrocyte  $\text{Ca}^{2+}$  influx through TrpA1 channels suppresses neuronal activity. **A**, All Alrm > TrpA1 flies became paralyzed within 30 s of exposure to  $33^\circ\text{C}$ , while control flies (Alrm-Gal4) show no behavioral defects.  $n > 80$  flies per genotype;  $p^a < 0.0001$ . **B**, Time course of paralysis in adult flies of the indicated genotypes on exposure to  $33^\circ\text{C}$ ; repo-Gal80 suppresses the paralysis in Alrm > TrpA1 background, while elav-Gal80 has no effect.  $n > 70$  flies for each genotype. **C**, Sample traces of CPG recording from larval NMJs. Postsynaptic potentials in Alrm > TrpA1 animals diminish during a temperature ramp from room temperature ( $22^\circ\text{C}$ ) to  $34^\circ\text{C}$ , while Alrm-Gal4 larvae maintain normal activity.

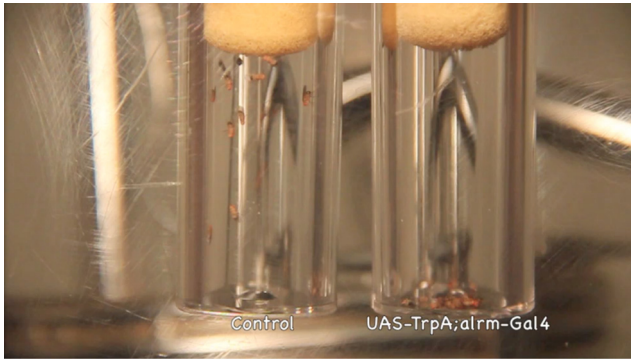
when the dissections were completed in  $<5$  min, and extreme care was taken to avoid damage to the CNS, astrocyte microdomain  $\text{Ca}^{2+}$  transients were rarely observed. Because these spontaneous astrocyte  $\text{Ca}^{2+}$  events were very sensitive to injury, we conducted  $\text{Ca}^{2+}$  imaging experiments in live, undissected L2 stage larvae that were confined between cover slips (see Materials and Methods).

Astrocyte near-membrane  $\text{Ca}^{2+}$  transients had an average duration of  $3.69 \pm 0.24$  s, a half decay time of  $1.00 \pm 0.06$  s, and a mean  $\Delta F/F_{\text{avg}}$  of  $34.30 \pm 1.70\%$  ( $n = 46$  individual  $\text{Ca}^{2+}$  oscillatory events). These events were similar to  $\text{Ca}^{2+}$  microdomains previously described in cortex glia, which had an average duration of 1.35 s, and a mean  $\Delta F/F_{\text{avg}}$  of 35% (Melom and Littleton, 2013). Recurrent  $\text{Ca}^{2+}$  transients within astrocyte processes were frequently observed in the same area (Fig. 1D), suggesting functional or structural subdomains where  $\text{Ca}^{2+}$  entry and removal are sequestered. Taken together, these results suggest that *Drosophila* astrocytes exhibit spontaneous  $\text{Ca}^{2+}$  oscillations that are similar to those previously described in cortex glia.

#### Acute astrocyte $\text{Ca}^{2+}$ influx via ectopic TRPA1 activation leads to paralysis

It has previously been shown that mutations in *zyd*, a *Drosophila* glial-specific  $\text{K}^+$ -dependent  $\text{Na}^+/\text{Ca}^{2+}$  ex-

changer (NCKX), led to elevated intracellular  $\text{Ca}^{2+}$  in cortex glia and enhanced seizure susceptibility, suggesting a role for glial  $\text{Ca}^{2+}$  signaling in regulating neuroexcitability (Melom and Littleton, 2013). We were interested in whether astrocyte  $\text{Ca}^{2+}$  signaling also regulates neural activity similar to that observed for cortex glia. To test this model, we used transgenic flies expressing TrpA1, a temperature-sensitive  $\text{Ca}^{2+}$  channel, under the control of a UAS promoter (UAS-TrpA1; Hamada et al., 2008). Prior studies expressing TrpA1 in cortex glia demonstrated this manipulation resulted in acute and robust seizure activity in neurons, with epileptic behavior observed in both larval and adult flies. When expressed using the astrocyte driver Alrm-Gal4, transgenic flies did not show any abnormality at room temperature ( $\sim 22^\circ\text{C}$ ). Strikingly, these animals became paralyzed within  $\sim 30$  s when acute  $\text{Ca}^{2+}$  influx was induced by shifting the temperature to  $33^\circ\text{C}$ , whereas control flies did not show any obvious behavioral defects (Fig. 2A; Movie 2). Similarly, acute astrocyte  $\text{Ca}^{2+}$  influx led to paralysis in 3rd instar stage Alrm > TrpA1 larvae but not in control animals (Movie 3). Pan-glial expression of Gal80, a Gal4 inhibitor, suppressed the paralysis in Alrm > TrpA1 flies, whereas pan-neuronal expression of Gal80 had no effect, indicating the observed paralysis was caused by acute  $\text{Ca}^{2+}$  influx into astrocytes rather than leaky expression in neurons (Fig. 2B).



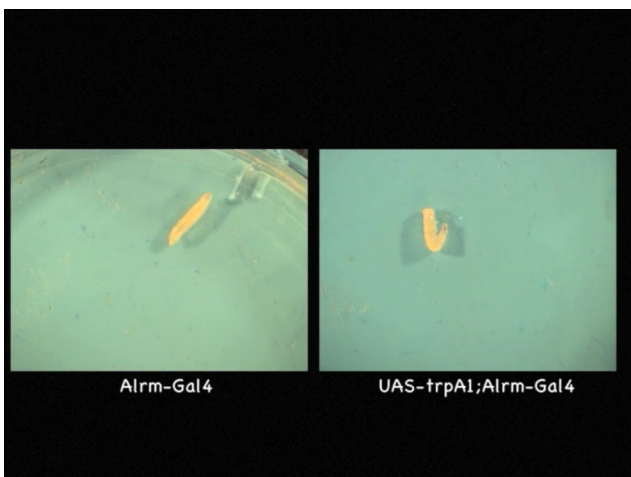
**Movie 2.** Astrocyte  $Ca^{2+}$  influx leads to suppression of neuronal activity in adult flies. Acute paralysis was induced in Alrm > TrpA1 flies when transferred to preheated water bath held at 33°C; control flies did not show obvious behavioral deficit. Video speed is real time.



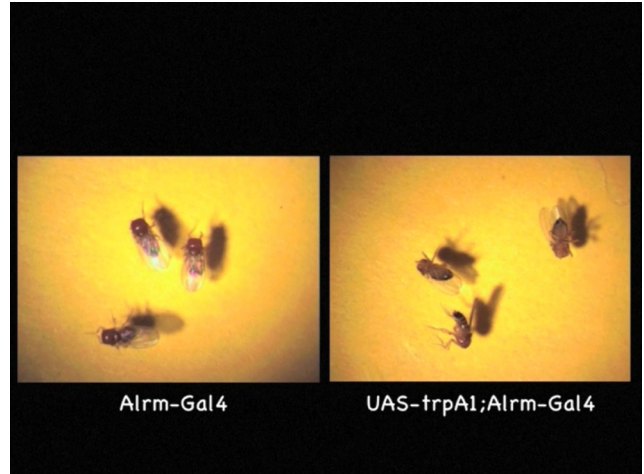
We next recorded CPG activity from the neuromuscular junction (NMJ) of 3rd instar stage larvae. Both control and Alrm > TrpA1 animals demonstrated normal spaced bursting activity that underlies larval locomotion at room temperature (Fig. 2C). However, when the temperature was ramped from ~22°C to ~34°C, neuronal activity in the Alrm > TrpA1 animals quickly diminished, whereas controls were unaffected (Fig. 2C). In contrast to cortex glia, our data indicate that acute astrocyte  $Ca^{2+}$  influx suppresses neuronal activity and leads to paralysis.

**Acute astrocyte  $Ca^{2+}$  influx-induced paralysis does not require central brain function**

In *Drosophila*, astrocytes extend fine processes and associate with synapses in the neuropil of both the central brain and the ventral ganglion (Muthukumar et al., 2014).



**Movie 3.** Acute astrocyte  $Ca^{2+}$  influx leads to paralysis in *Drosophila* larvae. Third instar Alrm > TrpA1 larvae rapidly lose voluntary muscle contraction and became paralyzed following transfer to a preheated Petri dish held at 34°C. Control larvae show enhanced locomotion activity. Video speed is real time.



**Movie 4.**  $Ca^{2+}$  influx in adult ventral ganglion astrocytes causes paralysis. Headless adult Alrm > TrpA1 flies show paralysis when transfer to a preheated Petri dish held at 33°C. The video started 30 s after the flies were transferred to the Petri dish. Video speed is real time.



The ventral ganglion is sufficient for conveying many motor functions. Headless flies with intact ventral ganglion survive for many hours and maintain posture, walk, and can learn to avoid electric shock (Booker and Quinn, 1981). It is possible that acute  $Ca^{2+}$  influx into astrocytes could suppress central brain function and cause motor impairment through descending neural circuit(s). Alternatively, the observed paralysis could be the consequence of direct interactions between astrocytes and local neurons in the ventral ganglion. To determine whether central brain function is necessary for conveying the astrocyte  $Ca^{2+}$  influx-induced paralysis, we severed the heads of adult flies and performed behavioral tests on headless flies. Headless flies expressing TrpA1 in astrocytes rapidly became paralyzed when the temperature was shifted to 33°C (Movie 4). Therefore, acute  $Ca^{2+}$  influx in astrocytes within the ventral ganglion is sufficient to trigger paralysis; central brain function is dispensable for this process.

**A candidate screen for modifiers of astrocyte  $Ca^{2+}$  influx-induced paralysis reveals a key role for Rab11 in GAT trafficking**

To understand the mechanism of acute astrocyte  $Ca^{2+}$  influx-induced suppression of neuronal activity, we conducted a candidate RNAi screen to identify modifiers of the paralysis phenotype of Alrm > TrpA1 flies. Candidate UAS-RNAi constructs were expressed in astrocytes by crossing with Alrm > TrpA1 flies, and the progeny were subjected to behavioral analysis in vials placed in a heated water bath. The screen was conducted at a lower temperature of 30°C, at which ~80% of the Alrm > TrpA1 became paralyzed, so that both suppressors and enhancers of motor impairment could be identified. We assembled a collection of ~140 RNAi lines for proteins that are (1) involved in vesicle transport, (2) enriched in astrocytes, or (3) involved in regulation of  $Ca^{2+}$  signaling. Using this

**Table 2: A screen for modifiers of the TS paralysis phenotype of Alrm > TrpA1 flies**

Gene product	CG no.	Effect	Function	RNAi stock no.
Esyt2	CG6643	Enhance	ER-PM tethering	v28418, v28419
SCAMP	CG9195	Enhance	SV trafficking	v9130
Nep4	CG4058	Enhance	Metalloendopeptidase	v16669, v100189
Syt4	CG10047	Suppress	Vesicle trafficking	v33317, BL26730
Syx1A	CG31136	Suppress	SNARE; Vesicle trafficking	v33113
Syt12	CG10617	Suppress	Vesicle trafficking	v47503
$\alpha$ -SNAP	CG6625	Suppress	SNARE disassembly	v101341, BL29587
Rab11	CG5771	Suppress	Endosome trafficking	v22198, BL27730

collection, we identified 13 RNAi lines that either enhanced or suppressed the motor impairments of Alrm > TrpA1 flies (Table 2).

Among the RNAi lines that suppressed the paralysis phenotype of Alrm > TrpA1 flies, Rab11-knockdown displayed the strongest effect (Fig. 3A; Alrm > TrpA1:  $87.92 \pm 2.043\%$ ; Alrm > TrpA1, Rab11-RNAi:  $31.12 \pm 4.813\%$ ;  $n > 100$  flies for both groups;  $p^b < 0.0001$ ). We verified the RNAi knockdown result using a dominant-negative mutant form of Rab11, Rab11<sup>N124I</sup> (Satoh et al., 2005). Overexpression of UAS-Rab11<sup>N124I</sup> in astrocytes resulted in a comparable suppression of the paralysis in Alrm > TrpA1 flies (Fig. 3B; Alrm > TrpA1:  $80.56 \pm 7.425\%$ ; Alrm > TrpA1, Rab11-DN:  $3.75 \pm 2.192\%$ ;  $n > 45$  flies for both groups;  $p^c = 0.0095$ ). Rab11 is a member of the Rab family of small-GTPases, and it is crucial for recycling endosome function and post-Golgi transport (Welz et al., 2014). It is possible that the reduced susceptibility to paralysis after suppression of Rab11 function in astrocytes is a result of impaired TrpA1 transport to astrocyte membranes and hence reduced Ca<sup>2+</sup> influx on temperature shifts. However, following expression of a UAS-TrpA1-myc transgene, we did not observe alteration in TrpA1-Myc localization (Fig. 3C) or intensity with *rab11* knockdown (Fig. 3D; control:  $1 \pm 0.0903$ , Rab11-RNAi:  $0.9323 \pm 0.0764$ ,  $n = 8$  single optical sections for each group,  $p^d = 0.5761$ ).

One of the major functions of astrocytes is to uptake neurotransmitters following synaptic activity (Eulenburg and Gomez, 2010). *Drosophila* astrocytes express GAT, the transporter responsible for synaptic clearance of the major inhibitory neurotransmitter GABA (Stork et al., 2014). It has been shown that membrane GAT levels are highly dynamic, and changes in GAT level can regulate neuronal excitability (Wang and Quick, 2005; Muthukumar et al., 2014). If GAT function or surface levels were suppressed by Ca<sup>2+</sup> influx into astrocytes, one might predict an acute behavioral paralysis due to high synaptic GABA levels and a general suppression of neuronal excitability. We tested whether suppression of Rab11 alters the transport or localization of GAT. Indeed, Rab11-knockdown in astrocytes led to accumulation of large amounts of GAT-containing vesicles in the cytoplasm, although GAT is normally predominantly localized to the plasma membrane (Fig. 3E). Overexpression of Rab11<sup>N124I</sup> caused a similar defect in GAT localization (Fig. 3E). We also assayed whether suppression of Rab11 function altered the overall level of GAT. Compared with controls, *rab11*-knockdown animals have similar levels of overall GAT

(Fig. 3F,G; control: 1, Rab11-RNAi:  $0.8368 \pm 0.1102$ ,  $n = 6$  experiments,  $p^e = 0.3125$ ). These data suggest that Rab11 is a novel regulator of GAT trafficking and likely ameliorates the acute astrocyte Ca<sup>2+</sup> influx-induced paralysis of Alrm > TrpA1 flies by indirectly regulating GABA uptake.

### Acute astrocyte Ca<sup>2+</sup> influx leads to reduced membrane GAT

At room temperature, Alrm > TrpA1 larvae display normal GAT expression and localization to astrocyte plasma membrane processes (Fig. 4A,B; Alrm-Gal4:  $1 \pm 0.03759$ , Alrm > TrpA1:  $1.051 \pm 0.06748$ ,  $n = 8-10$  single optical sections for each group,  $p^f = 0.4974$ ). However, after subjecting animals to 33°C, Alrm > TrpA1 larvae showed a severe reduction of surface GAT expression compared with controls (Fig. 4A,B; Alrm-Gal4:  $1 \pm 0.06333$ , Alrm > TrpA1:  $0.4451 \pm 0.05023$ ,  $n = 8$  single optical sections for each group,  $p^g < 0.0001$ ). Large, GAT-containing membranous structures were frequently observed in the cytoplasm following acute Ca<sup>2+</sup> influx in astrocytes, indicating Ca<sup>2+</sup> elevation may drive GAT endocytosis (Fig. 4C).

These results suggest a Ca<sup>2+</sup>-dependent endocytotic pathway dynamically regulates membrane GAT levels. We hypothesize that excessive synaptic GABA due to the reduction in astrocyte surface GAT levels triggers the Ca<sup>2+</sup> influx-induced paralysis. To test whether increased GABAergic signaling could lead to rapid paralysis, we expressed TrpA1 using a GABAergic neuron driver, GAD1-Gal4 (Ng et al., 2002). These flies became paralyzed within ~30 s after being transferred to 30°C, indicating excessive GABA synaptic levels result in a strong suppression of neuronal activity and rapid behavioral paralysis in *Drosophila* (Fig. 5A).

## Discussion

In the present study, we investigated Ca<sup>2+</sup> influx in *Drosophila* astrocytes and the role of astrocyte Ca<sup>2+</sup> signals in regulating neuronal activity. We found that similar to cortex glia (Melom and Littleton, 2013), *Drosophila* astrocytes exhibit spontaneous Ca<sup>2+</sup> transients. However, in contrast to cortex glia, acute astrocyte Ca<sup>2+</sup> influx leads to suppression of neuronal activity. Elevated cytoplasmic Ca<sup>2+</sup> in astrocytes is associated with fast endocytosis of GAT and a reduction in surface expression, which is likely to disrupt GABA uptake and induce rapid paralysis. Suppression of Rab11 led to a disruption in GAT distribution and ameliorated the paralysis caused by astrocyte Ca<sup>2+</sup> influx, revealing a novel mechanism of

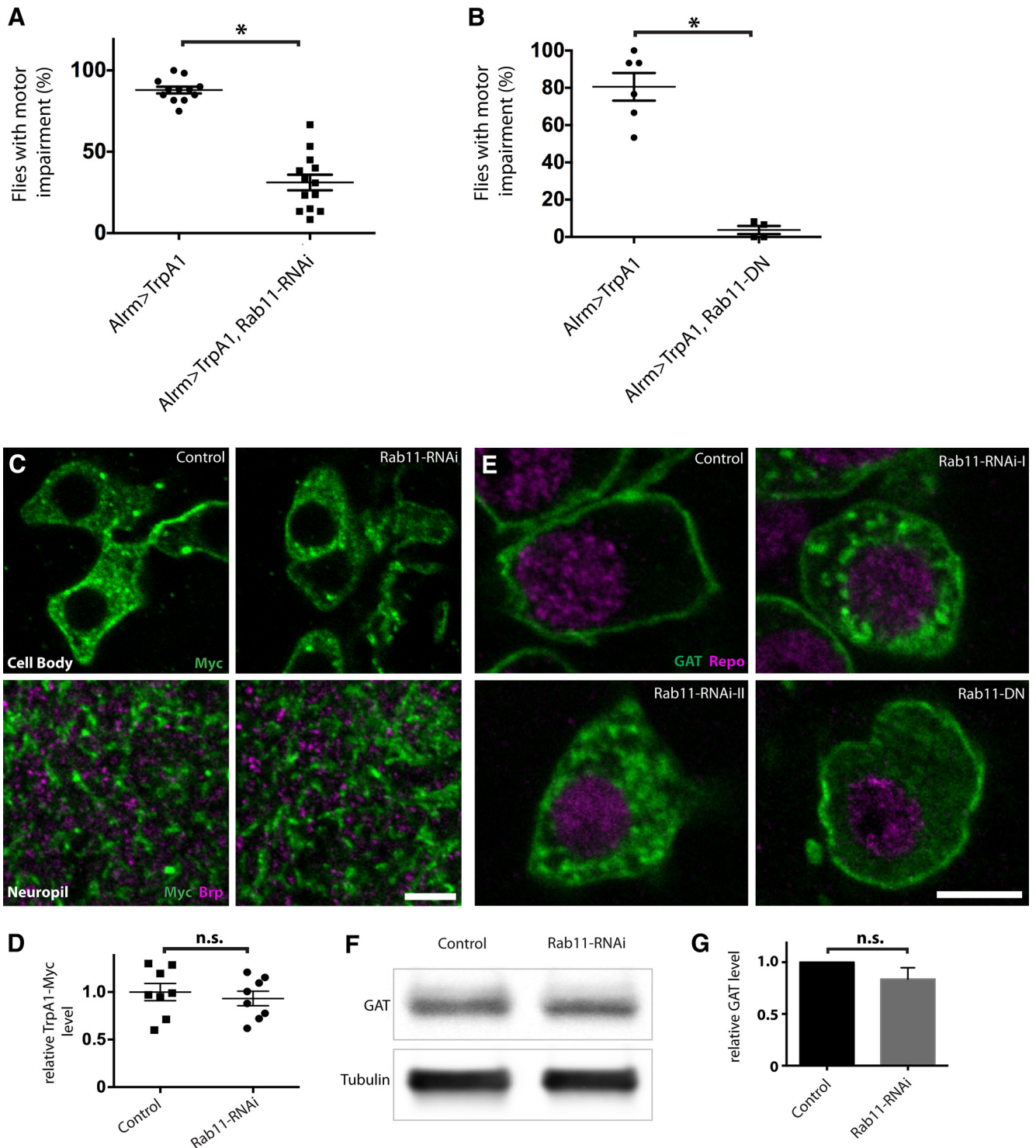


**Figure 3.** Suppression of Rab11 function ameliorates astrocyte  $Ca^{2+}$  influx-induced behavioral defects and impairs GAT trafficking. **A**, Quantification of paralyzed flies when exposed to  $30^{\circ}C$ , showing *rab11*-knockdown suppressed the paralysis in *Alrm > TrpA1* flies.  $n > 100$  flies per genotype;  $p^b < 0.00001$ . **B**, Quantification of paralyzed flies when *Alrm > TrpA1* and *Alrm > TrpA1, Rab11-DN* flies were transferred to  $30^{\circ}C$ .  $n > 45$  flies per genotype;  $p^c = 0.0095$ . **C**, Single optical section showing astrocyte cell body and neuropil in the VNCs of *Alrm > TrpA1-myc* (control) and *Alrm > TrpA1-myc, Rab11-RNAi* (*Rab11-RNAi*) larvae stained with antibodies against Myc (green) and Brp (magenta). Note the apposition between synapses and astrocyte processes in the neuropil. **D**, Quantification of relative *TrpA1-Myc* level, normalized to control.  $n = 8$  individual optical planes for each group;  $p^d = 0.5761$ . **E**, Optical sections showing GAT localization in astrocytes of larval VNCs stained with antibodies against GAT (green) and Repo (magenta) in control and when *Rab11-RNAi* or *Rab11-DN* is expressed in astrocytes. **F**, Western blotting of adult heads showing the effect of *Rab11-RNAi* expression in astrocytes on GAT level. **G**, Quantification of **F**.  $n = 6$  experiments;  $p^e = 0.3125$ . Scale bars in **C** and **E**,  $5 \mu m$ .



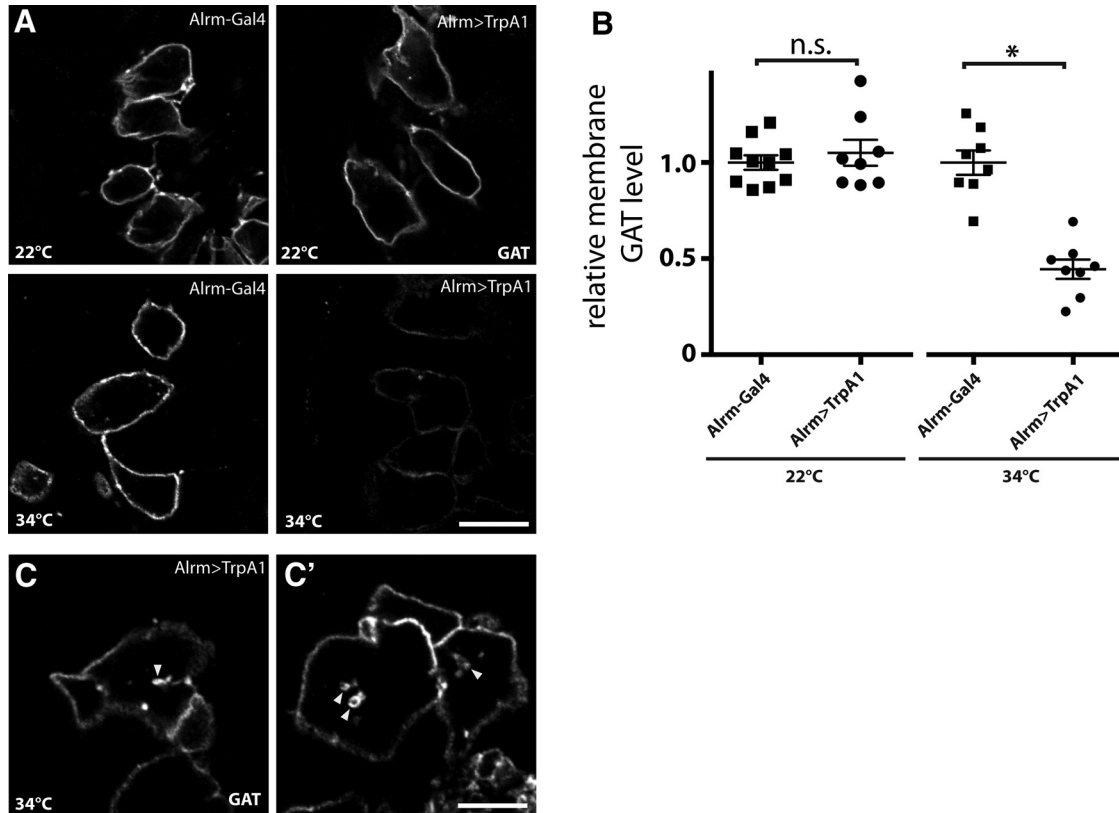


**Figure 4.** Astrocyte  $Ca^{2+}$  influx leads to reduced membrane GAT. **A**, Confocal images of larval VNC showing astrocyte membrane GAT level in control and Alrm > TrpA1 animals at room temperature (22°C) or 34°C. **B**, Quantification of relative GAT level shown in **A**, normalized to Alrm-Gal4 animals at each temperature.  $n = 8-10$  individual optical planes for all groups;  $p^f = 0.4974$  and  $p^g < 0.0001$ , respectively. **C**, **C'**, Confocal images with longer exposure showing GAT-containing vesicles (arrowheads) forming in the cytoplasm of Alrm > TrpA1 larvae exposed to 34°C. Scale bars in **A** and **C**, 5  $\mu m$ .

Rab11-dependent control of membrane GAT and neuronal activity.

**Drosophila astrocytes demonstrate spontaneous microdomain  $Ca^{2+}$  activity**

Current data indicate that astrocytes display diverse forms of intracellular  $Ca^{2+}$  oscillations through distinct cellular mechanisms (Bazargani and Attwell, 2016). Changes in astrocyte  $Ca^{2+}$  levels could be a response to neuronal activity. In isolated rat retinas, light flashing causes an increase in  $Ca^{2+}$  in retinal glial cells (Newman, 2005). In the cortex of anesthetized mice, astrocytes were also found to elevate intracellular  $Ca^{2+}$  in response to whisker stimulation (Wang et al., 2006). However, the  $Ca^{2+}$  oscillatory activities that we observe in *Drosophila* astrocytes appear to more closely resemble another form of fast, microdomain  $Ca^{2+}$  fluctuation, which has not yet been demonstrated to correlate with neuronal activity. In a rodent neuron-astrocyte coculture system,  $Ca^{2+}$  oscillations in astrocytes appeared to be mediated by spontaneous opening of TRPA1 channels independent of neuronal spiking (Shigetomi et al., 2012). Another study using acute mouse hippocampal brain slices also showed that pharmacological blockage of neuronal activity did not affect either the frequency or the amplitude of localized  $Ca^{2+}$  transients at fine processes of CA1 astrocytes (Rungta et al., 2016).

It is interesting that  $Ca^{2+}$  oscillations in *Drosophila* astrocytes bear remarkable similarity with those observed in cortex glia (Melom and Littleton, 2013), despite the distinction in the morphology between these two types of glial cells. The similar patterns of  $Ca^{2+}$  oscillations may suggest a common cellular mechanism for their origin. Unlike astrocytes, cortex glia cells are segregated from the synaptic neuropil and, instead, enwrap neuronal cell bodies in the cortex region of the CNS with their thin processes (Ito et al., 1995). It is unclear whether cortex glial might directly sense neuronal activity as a trigger for  $Ca^{2+}$  oscillations due to their lack of direct contact with chemical synapses. With the caveat that we could not use pharmacological methods to directly test the origin of astrocyte  $Ca^{2+}$  transients due to their sensitivity to injury, these microdomain  $Ca^{2+}$  fluctuations are likely a result of spontaneous glial channel opening rather than being directly triggered by neuronal activity.

**Distinct functions of glial  $Ca^{2+}$  signals on neuronal activity**

We find that acute  $Ca^{2+}$  influx into astrocytes leads to suppression of neuronal activity, an effect opposite to the enhancement of neuronal firing following elevated cortex glia  $Ca^{2+}$  signaling (Melom and Littleton, 2013). Although the exact mechanism is unclear, increased cortex glial  $Ca^{2+}$  level may trigger excessive neuronal activity through

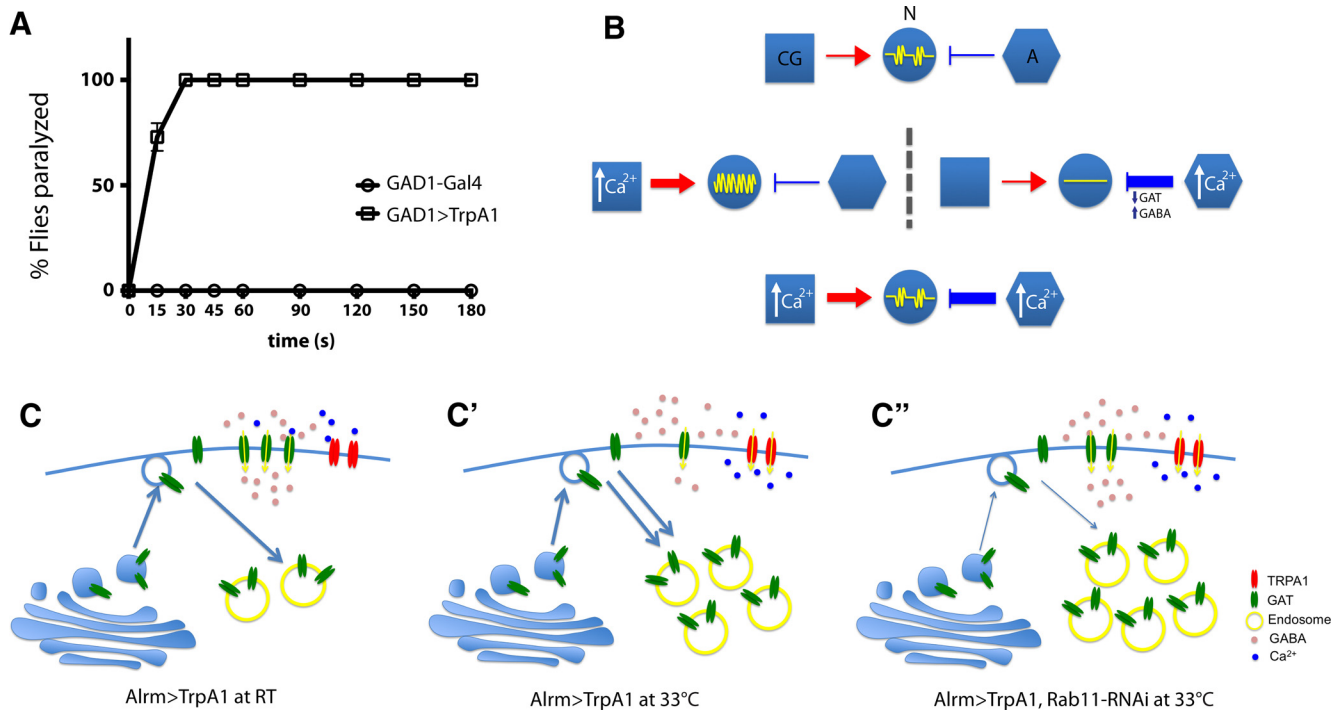


**Figure 5.** Excessive GABA leads to suppression of neuronal activity. **A**, Quantification of paralyzed flies on exposure to 30°C. Ectopic activation of GABAergic neurons via GAD1-Gal4-induced expression of TrpA1 leads to acute suppression of neuronal activity and paralysis. **B**, Distinct impact of cortex glia and astrocyte  $Ca^{2+}$  signals on neuronal activity.  $Ca^{2+}$  influx in cortex glia leads to increased neural activity and seizure-like behavior, whereas enhanced astrocyte  $Ca^{2+}$  signal causes suppression of neuronal activity and paralysis. Together, they constitute a  $Ca^{2+}$ -dependent glial mechanism to fine-tune neuronal function. **C-C''**, Model of how astrocyte  $Ca^{2+}$  signaling regulates neuronal activity. Astrocyte  $Ca^{2+}$  influx leads to acute endocytosis of membrane GAT, reduced GABA uptake, and suppression of neuronal activity. Inhibition of Rab11 function reduces the removal of membrane GAT and sustains GABA uptake, hence ameliorating the paralysis caused by astrocyte  $Ca^{2+}$  influx.

their ability to influence the environment around neuronal cell bodies, or through gliotransmission that activates surface receptors on neuronal cell bodies. Based on our results, astrocyte  $Ca^{2+}$  influx appears to balance cortex glia excitation through inhibition of neuronal activity, and together they constitute a glial mechanism to fine-tune the balance between excitatory and inhibitory signals to maintain normal neuronal excitability (Fig. 5B).

Perturbations in glial  $Ca^{2+}$  activity have been implicated in several forms of neurologic disorders (Nedergaard et al., 2010; Shigetomi et al., 2016). For example, it was found that both the basal astrocyte  $Ca^{2+}$  level and the frequency of somatic  $Ca^{2+}$  activity increase in a mouse model of Alzheimer’s disease, which might contribute to alterations in brain function (Kuchibhotla et al., 2009). Although we did not find evidence that the transient induction of astrocyte  $Ca^{2+}$  influx used in our study resulted in long-lasting pathology (data not shown), it will be interesting to explore the role of chronic increases in glial  $Ca^{2+}$  signals in the pathogenesis of neurologic diseases using the *Drosophila* model.

In the *Drosophila* CNS, astrocytes invade the entire neuropil with their meshwork of fine processes, and each astrocyte establishes unique and stereotypical territory (Muthukumar et al., 2014; Stork et al., 2014). Although much is known about the distinct origin and functions of astrocytes in different mammalian brain regions (Bayrak-

tar et al., 2014), the functional heterogeneity and/or redundancy of astrocytes in *Drosophila* is still largely unexplored. Here, as a first step, we show that astrocytes in the ventral ganglion are sufficient to convey the suppression of neuronal activity caused by acute  $Ca^{2+}$  influx.

**A mechanism regulating astrocyte membrane GAT and neuroactivity**

Modulation of GABA uptake is an important glial mechanism to actively participate in the regulation of neuronal activity. It has been previously shown that global GAT levels in *Drosophila* astrocytes are developmentally regulated and sensitive to GABAergic neuronal output during synaptogenesis (Muthukumar et al., 2014). Suppression of metabotropic GABA<sub>B</sub> receptor signaling reduces GAT levels and suppresses seizure induction in hyperexcitable *Drosophila* seizure mutants, likely through dampening the rate of GABA uptake (Muthukumar et al., 2014).

Our study suggests the existence of a new mechanism for astrocytes to acutely regulate neuronal activity through fast modulation of GAT turnover. Compared with other known membrane proteins, GAT has one of the highest turnover rates (Tanner and Lienhard, 1987; Harwood and Pellarin, 1997; Menne et al., 2002; Wang and Quick, 2005). Plasma membrane GAT levels are dynamically regulated via a balance between fast endocytosis and exocytosis in primary rat cortical neuron cultures (Wang and

Quick, 2005). Pharmacological activation of protein kinase C (PKC) can trigger enhanced endocytosis of GAT, leading to reduced membrane expression and reduction in GABA uptake (Wang and Quick, 2005). Here, our results suggest that astrocyte  $\text{Ca}^{2+}$  influx induces a rapid decrease in membrane GAT levels via endocytosis, which correlates with acute suppression of neural activity, representing a mechanism for glial cells to actively modulate neuronal function.

Our data reveal Rab11 as a novel regulator of GAT trafficking in *Drosophila* astrocytes. The accumulation of GAT-containing vesicles in *rab11*-knockdown animals likely represents a strong suppression of post-Golgi transport of GAT to the plasma membrane. However, it is important to note that suppression of Rab11 function did not totally abolish GAT localization to astrocyte membranes (Fig. 3D). Consistently, *rab11*-knockdown flies do not have strong locomotion defects like GAT-deficient animals (Stork et al., 2014). Indeed, it has been shown that GAT is delivered to the plasma membrane via multiple pathways (Reiterer et al., 2008). Since *rab11*-knockdown did not alter total GAT levels (Fig. 3E,F), constitutive membrane GAT in these animals seems sufficient to support baseline GABA uptake. Although primarily considered a regulator of recycling endosomes, Rab11 has been shown to promote endocytosis through indirect mechanisms. In the *Drosophila* eye, suppression of Rab11 function decreases the rate of endocytosis and eliminates the formation of endocytosis-dependent multivesicular bodies (Satoh et al., 2005). Ectopic expression of a dominant negative form of Rab11 also disrupts endocytosis in cultured *Drosophila* Garland cells (Satoh et al., 2005). Consistent with these observations, our data support a model in which suppression of Rab11 function blocks GAT endocytosis triggered by astrocyte  $\text{Ca}^{2+}$  influx, leading to sustained GABA uptake and a suppression of the paralysis and loss of neural activity normally observed following excessive astrocyte  $\text{Ca}^{2+}$  influx (Fig. 5C).

Taken together, our study reveals an important function of glial  $\text{Ca}^{2+}$  signaling in regulating neuronal activity. Acute modulation of the rate of neurotransmitter uptake through  $\text{Ca}^{2+}$ -dependent glial signaling provides a robust mechanism for astrocytes to actively modulate the function of neural circuits.

## References

- Agulhon C, Fiacco TA, McCarthy KD (2010) Hippocampal short- and long-term plasticity are not modulated by astrocyte  $\text{Ca}^{2+}$  signaling. *Science* 327:1250–1254. [CrossRef Medline](#)
- Alvarez-Maubecin V, Garcia-Hernandez F, Williams JT, Van Bockstaele EJ (2000) Functional coupling between neurons and glia. *J Neurosci* 20:4091–4098. [Medline](#)
- Awasaki T, Lai SL, Ito K, Lee T (2008) Organization and postembryonic development of glial cells in the adult central brain of *Drosophila*. *J Neurosci* 28:13742–13753. [CrossRef Medline](#)
- Bayraktar OA, Fuentealba LC, Alvarez-Buylla A, Rowitch DH (2014) Astrocyte development and heterogeneity. *Cold Spring Harb Perspect Biol* 7:a020362. [CrossRef Medline](#)
- Bazargani N, Attwell D (2016) Astrocyte calcium signaling: the third wave. *Nat Neurosci* 19:182–189. [CrossRef Medline](#)
- Booker R, Quinn WG (1981) Conditioning of leg position in normal and mutant *Drosophila*. *Proc Natl Acad Sci USA* 78:3940–3944. [Medline](#)
- Carvill GL, McMahon JM, Schneider A, Zemel M, Myers CT, Saykally J, Nguyen J, Robbiano A, Zara F, Specchio N, Mecarelli O, Smith RL, Leventer RJ, Moller RS, Nikanorova M, Dimova P, Jordanova A, Petrou S, EuroEPINOMICS Rare Epilepsy Syndrome Myoclonic-Astatic Epilepsy & Dravet working group, Helbig I, et al. (2015) Mutations in the GABA transporter SLC6A1 cause epilepsy with myoclonic-atonic seizures. *Am J Hum Genet* 96:808–815. [Cross-Ref](#)
- Cornell-Bell AH, Finkbeiner SM, Cooper MS, Smith SJ (1990) Glutamate induces calcium waves in cultured astrocytes: long-range glial signaling. *Science* 247:470–473. [Medline](#)
- Dani JW, Chernjavsky A, Smith SJ (1992) Neuronal activity triggers calcium waves in hippocampal astrocyte networks. *Neuron* 8:429–440. [Medline](#)
- Dietzl G, Chen D, Schnorrer F, Su KC, Barinova Y, Fellner M, Gasser B, Kinsey K, Oettel S, Scheiblauer S, Couto A, Marra V, Keleman K, Dickson BJ (2007) A genome-wide transgenic RNAi library for conditional gene inactivation in *Drosophila*. *Nature* 448:151–156. [CrossRef Medline](#)
- Doherty J, Logan MA, Taşdemir OE, Freeman MR (2009) Ensheathing glia function as phagocytes in the adult *Drosophila* brain. *J Neurosci* 29:4768–4781. [CrossRef Medline](#)
- Eulenburg V, Gomez J (2010) Neurotransmitter transporters expressed in glial cells as regulators of synapse function. *Brain Res Rev* 63:103–112. [CrossRef Medline](#)
- Feng Y, Ueda A, Wu CF (2004) A modified minimal hemolymph-like solution, HL3.1, for physiological recordings at the neuromuscular junctions of normal and mutant *Drosophila* larvae. *J Neurogenet* 18:377–402. [CrossRef Medline](#)
- Freeman MR (2015) *Drosophila* Central Nervous System Glia. *Cold Spring Harb Perspect Biol*
- Hamada FN, Rosenzweig M, Kang K, Pulver SR, Ghezzi A, Jegla TJ, Garrity PA (2008) An internal thermal sensor controlling temperature preference in *Drosophila*. *Nature* 454:217–220. [CrossRef Medline](#)
- Harada K, Kamiya T, Tsuboi T (2015) Gliotransmitter release from astrocytes: functional, developmental, and pathological implications in the brain. *Front Neurosci* 9:499. [CrossRef Medline](#)
- Harwood HJ Jr, Pellarin LD (1997) Kinetics of low-density lipoprotein receptor activity in Hep-G2 cells: derivation and validation of a Briggs-Haldane-based kinetic model for evaluating receptor-mediated endocytotic processes in which receptors recycle. *Biochem J* 323:649–659. [CrossRef](#)
- Henneberger C, Papouin T, Oliet SH, Rusakov DA (2010) Long-term potentiation depends on release of D-serine from astrocytes. *Nature* 463:232–236. [CrossRef Medline](#)
- Ito K, Urban J, Technau GM (1995) Distribution, classification, and development of *Drosophila* glial cells in the late embryonic and early larval ventral nerve cord. *Roux's Archive in Developmental Biology* 204:284–307. [CrossRef](#)
- Kremer MC, Jung C, Batelli S, Rubin GM, Gaul U (2017) The glia of the adult *Drosophila* nervous system. *Glia* 65:606–638.
- Kuchibhotla KV, Lattarulo CR, Hyman BT, Bacskaï BJ (2009) Synchronous hyperactivity and intercellular calcium waves in astrocytes in Alzheimer mice. *Science* 323:1211–1215. [CrossRef Medline](#)
- Ma Z, Stork T, Bergles DE, Freeman MR (2016) Neuromodulators signal through astrocytes to alter neural circuit activity and behaviour. *Nature* 539:428–432. [CrossRef Medline](#)
- Melom JE, Littleton JT (2013) Mutation of a NCKX eliminates glial microdomain calcium oscillations and enhances seizure susceptibility. *J Neurosci* 33:1169–1178. [CrossRef Medline](#)
- Menne C, Møller Sørensen T, Siersma V, von Essen M, Ødum N, Geisler C (2002) Endo- and exocytic rate constants for spontaneous and protein kinase C-activated T cell receptor cycling. *Eur J Immunol* 32:616–626. [CrossRef Medline](#)

- Minelli A, DeBiasi S, Brecha NC, Zuccarello LV, Conti F (1996) GAT-3, a high-affinity GABA plasma membrane transporter, is localized to astrocytic processes, and it is not confined to the vicinity of GABAergic synapses in the cerebral cortex. *J Neurosci* 16:6255–6264.
- Muthukumar AK, Stork T, Freeman MR (2014) Activity-dependent regulation of astrocyte GAT levels during synaptogenesis. *Nat Neurosci* 17:1340–1350. [CrossRef Medline](#)
- Nedergaard M (1994) Direct signaling from astrocytes to neurons in cultures of mammalian brain cells. *Science* 263:1768–1771. [Medline](#)
- Nedergaard M, Rodríguez JJ, Verkhratsky A (2010) Glial calcium and diseases of the nervous system. *Cell Calcium* 47:140–149. [Cross-Ref Medline](#)
- Newman EA (2005) Calcium increases in retinal glial cells evoked by light-induced neuronal activity. *J Neurosci* 25:5502–5510. [Cross-Ref Medline](#)
- Ng M, Roorda RD, Lima SQ, Zemelman BV, Morcillo P, Miesenböck G (2002) Transmission of olfactory information between three populations of neurons in the antennal lobe of the fly. *Neuron* 36:463–474. [Medline](#)
- Parpura V, Basarsky TA, Liu F, Jęftinija K, Jęftinija S, Haydon PG (1994) Glutamate-mediated astrocyte-neuron signalling. *Nature* 369:744–747. [CrossRef Medline](#)
- Perkins LA, Holderbaum L, Tao R, Hu Y, Sopko R, McCall K, Yang-Zhou D, Flockhart I, Binari R, Shim HS, Miller A, Housden A, Foos M, Randkelv S, Kelley C, Namgyal P, Villalta C, Liu LP, Jiang X, Huan-Huan Q, et al. (2015) The transgenic RNAi project at Harvard Medical School: resources and validation. *Genetics* 201:843–852. [CrossRef Medline](#)
- Petravicz J, Fiacco TA, McCarthy KD (2008) Loss of IP3 receptor-dependent Ca<sup>2+</sup> increases in hippocampal astrocytes does not affect baseline CA1 pyramidal neuron synaptic activity. *J Neurosci* 28:4967–4973. [CrossRef](#)
- Reiterer V, Maier S, Sitte HH, Kriz A, Rüegg MA, Hauri HP, Freissmuth M, Farhan H (2008) Sec24- and ARFGAP1-dependent trafficking of GABA transporter-1 is a prerequisite for correct axonal targeting. *J Neurosci* 28:12453–12464. [CrossRef Medline](#)
- Rungta RL, Bernier LP, Dissing-Olesen L, Groten CJ, LeDue JM, Ko R, Drissler S, MacVicar BA (2016) Ca<sup>2+</sup> transients in astrocyte fine processes occur via Ca<sup>2+</sup> influx in the adult mouse hippocampus. *Glia* 64:2093–2103.
- Satoh AK, O'Tousa JE, Ozaki K, Ready DF (2005) Rab11 mediates post-Golgi trafficking of rhodopsin to the photosensitive apical membrane of *Drosophila* photoreceptors. *Development* 132:1487–1497. [CrossRef Medline](#)
- Scimemi A (2014) Structure, function, and plasticity of GABA transporters. *Front Cell Neurosci* 8:161. [CrossRef Medline](#)
- Shigetomi E, Jackson-Weaver O, Huckstepp RT, O'Dell TJ, Khakh BS (2013) TRPA1 channels are regulators of astrocyte basal calcium levels and long-term potentiation via constitutive D-serine release. *J Neurosci* 33:10143–10153. [CrossRef Medline](#)
- Shigetomi E, Kracun S, Sofroniew MV, Khakh BS (2010) A genetically targeted optical sensor to monitor calcium signals in astrocyte processes. *Nat Neurosci* 13:759–766. [CrossRef Medline](#)
- Shigetomi E, Patel S, Khakh BS (2016) Probing the complexities of astrocyte calcium signaling. *Trends Cell Biol* 26:300–312. [Cross-Ref Medline](#)
- Shigetomi E, Tong X, Kwan KY, Corey DP, Khakh BS (2012) TRPA1 channels regulate astrocyte resting calcium and inhibitory synapse efficacy through GAT-3. *Nat Neurosci* 15:70–80.
- Stork T, Sheehan A, Tasdemir-Yilmaz OE, Freeman MR (2014) Neuron-glia interactions through the heartless FGF receptor signaling pathway mediate morphogenesis of *Drosophila* astrocytes. *Neuron* 83:388–403. [CrossRef Medline](#)
- Tanner LI, Lienhard GE (1987) Insulin elicits a redistribution of transferrin receptors in 3T3-L1 adipocytes through an increase in the rate constant for receptor externalization. *J Biol Chem* 262:8975–8980. [Medline](#)
- Volterra A, Liaudet N, Savtchouk I (2014) Astrocyte Ca<sup>2+</sup> signalling: an unexpected complexity. *Nat Rev Neurosci* 15:327–335. [Cross-Ref Medline](#)
- von Philipsborn AC, Liu T, Yu JY, Masser C, Bidaye SS, Dickson BJ (2011) Neuronal control of *Drosophila* courtship song. *Neuron* 69:509–522. [CrossRef Medline](#)
- Wang D, Quick MW (2005) Trafficking of the plasma membrane gamma-aminobutyric acid transporter GAT1. Size and rates of an acutely recycling pool. *J Biol Chem* 280:18703–18709.
- Wang X, Lou N, Xu Q, Tian GF, Peng WG, Han X, Kang J, Takano T, Nedergaard M (2006) Astrocytic Ca<sup>2+</sup> signaling evoked by sensory stimulation in vivo. *Nat Neurosci* 9:816–823. [CrossRef Medline](#)
- Welz T, Wellbourne-Wood J, Kerkhoff E (2014) Orchestration of cell surface proteins by Rab11. *Trends Cell Biol* 24:407–415. [CrossRef Medline](#)
- Yang CH, Rumpf S, Xiang Y, Gordon MD, Song W, Jan LY, Jan YN (2009) Control of the postmating behavioral switch in *Drosophila* females by internal sensory neurons. *Neuron* 61:519–526. [Cross-Ref Medline](#)